Monte Carlo simulation of initial and volume ion recombination correction factor in plane parallel ionization chambers exposed to ion beams with clinical dose rates

M. Orts Sanz [1], S. Rossomme [4], K. Souris [4] and E. Sterpin [1,2,3]

[1] UCLouvain – Institut de Recherche Expérimentale et Clinique - Molecular Imaging Radiotherapy and Oncology (MIRO), Brussels, Belgium

[2] KU Leuven – Department of Oncology – Laboratory of Experimental Radiotherapy, Leuven, Belgium

[3] Particle Therapy Interuniversity Center Leuven – Particle, Leuven, Belgium

[4] Ion Beams Applications S.A., Dosimetry Business Unit, Louvain La Neuve, Belgium

0. Abstract

Purpose: Accurate dose determination with ionization chambers relies on correcting for various influencing factors, including ion recombination. Theoretical frameworks, such as the Boag and Jaffe theories, are conventionally used to describe the ion recombination correction factors. The development of simulation tools becomes necessary to enhance the understanding of recombination under circumstances that may differ from conventional use. Before progressing, it is crucial to benchmark novel approaches to calculate ion recombination losses under known conditions. In this study, we introduce and validate a versatile simulation tool based on a Monte Carlo scheme for calculating initial and volume ion recombination correction factors in air-filled ionization chambers exposed to ion beams with clinical dose rates.

Method: The simulation includes gaussian distribution of ions to model the distribution of charge carriers along the chamber volume. It accounts for various physical transport effects, including drift, diffusion, space charge screening and free electron fraction. To compute ion recombination, a Monte Carlo scheme is used due to its versatility in multiple geometries, without exhibiting convergence problems associated with numerically solved procedures.

Result: The code is validated in conventional dose rates against Jaffe's theory for initial recombination and Boag's theory for volume recombination based on parameters derived from experimental data including proton, helium and carbon ion beams measured with a plane parallel ionization chamber.

Conclusion: The code demonstrates excellent agreement, typically 0.05% or less relative difference with the theoretical and experimental data. The current code successfully predicts ion recombination correction factors, in a large variety of ion beams, including different temporal beam structures.

1. Introduction

Air filled ionization chambers (IC) are one of the most accurate and reliable dosimeters to determine the absorbed dose in radiotherapy. They are extensively used in clinics and international dosimetry codes of practice such as IAEA TRS-398 (Andreo et al., 2001) and AAPM TG-51 (Almond et al., 1999) endorse their use as the preferred detector for reference dosimetry and daily quality assurance in electron, photon, proton and heavier ion beams.

ICs measure the charged ion pairs created by the ionizing radiation inside the cavity of the detector. However, due to recombination, some of these ions do not reach the electrodes, leading to an underestimation of the collected charges. To compensate for this effect, an ion recombination correction factor (k_s) is applied to the response of the ionization chamber.

Ion recombination is a complex mechanism influenced by a variety of parameters, including particle type, beam quality, Linear Energy Transfer (LET), depth, voltage, dose rate, beam delivery method and ionization chamber design. Generally, two types of recombination are recognized: initial and volume recombination. Initial recombination (intra-track recombination) occurs between ions within the same track - same trail of ionized species left behind the incident radiation particle - and it is theoretically addressed in the Jaffe model (Jaffé, 1913). This type of recombination is heavily influenced by the LET of the particle. In contrast, volume or general recombination is produced between ions of different tracks (inter-track recombination). It is described in the Boag model (Boag, 1950) and is mainly dependent on the dose rate. In 1996, Boag extended his theory to account for the fraction of electrons that do not attach to other molecules (Boag et al., 1996), known as the “free electron effect”. There are three updated models, each of them corresponding to different approximations of the distribution of electrons inside the ionization chamber. All three models estimate lower recombination compared to the original expression and depend on the free electron fraction, p:

$$p = \frac{1}{ad}(1 - e^{-ad}) \quad (1)$$

being d the distance between electrodes in plane-parallel geometry and a a coefficient that depends on the gas and the electric field strength. This coefficient a can be calculated as the inverse of the product of the mean time until attachment of the electron and the drift velocity of the free electron in the gas. These values are dependent on the electric field (Laitano et al., 2006) and can be calculated from a fitting to the experimental data from (Huxley, 1974).

Several methods have been developed to experimentally determine k_s, among them, the widely known two-voltage method (TVM), the recent three-voltage method (3VM) by (Rossomme et al., 2020) or the approach developed by (Boutillon, 1998) based on (Niatel, 1967) and extended by (Palmans et al., 2006). The two-voltage method (TVM) is a reliable and accurate technique extensively tested and validated in electron and photon beams and is the standard method recommended by IAEA TRS-398 and AAPM TG-51. It is based on a first-order term of a series expansion around 1/V = 0 of Boag’s theory, in which the equation for k_s can be simplified as a

linear relation between k_s and the inverse of the applied voltage ($1/V$) for pulsed beams or $1/V^2$ for continuous beams. Due to this approximation, the TVM is only valid when the measured current is close to the saturation current.

For protons and ion beams, the dense track cores result in variations on charge distributions and the contribution of initial recombination can disturb this linearity (Palmans et al., 2006). In particle beams, the use of the TVM is often limited (Rossomme et al., 2020) and alternative methods such as (Boutillon, 1998) are needed. The Boutillon approach allows to determine experimentally the contribution of initial and volume recombination in a continuous beam by measuring the inverse of the charge measured by the IC versus the inverse of the voltage (these charts are frequently referred to as Jaffe plots) for three different dose rates. However, this method is time consuming and not feasible in clinical routine, leaving linear methods as the only practical way to account for recombination.

Simulations are an accurate and time-efficient tool to comprehend recombination losses in cases that deviate from the conditions in which experimental methods or theories were intended and may not be valid. They can also help to find strategies to minimize recombination by making easy to explore different combinations of geometry and applied voltage.

In recent years, various simulations have emerged, primarily based on the resolution of partial differential equation systems (PDEs) that describe the temporal evolution of charge within the IC. (Paz-Martín et al., 2022) accurately predicts the complex chamber response for electron beams by assuming a homogeneous distribution of ions and solving the PDEs in one dimension. However, this approach is not suitable to model ion beams because the non-uniform gaussian distribution does not allow the reduction of the dimensions of the problem. In (Christensen et al., 2016) the PDEs resolution is extended to three dimensions, allowing to model initial and volume recombination in proton beams.

However, when dealing with complex geometries, the election of the mesh to solve the DPEs may be challenging and, in low dose rate scenarios where low charge densities are present, convergence issues with the resolution of the PDEs may arise. To avoid these potential problems, (García et al., 2021) proposed a Monte Carlo simulation method that demonstrates its versatility across various geometries and any charge density distribution. However, their work focuses on modeling different geometries by assuming homogeneous ion distributions and exclusively models ion drift as the transport mechanism through the IC.

In this paper, we present a Monte Carlo based simulation to model k_s for light ion beams addressing both initial and volume recombination. The simulation includes Gaussian ion track structure and allows to generalize for any ion beam, energy spectrum and temporal structure of the beam. It includes transport mechanisms like drift, diffusion, free electron fraction and space charge screening. These last two effects, and especially the space charge screening, are believed to be crucial in the UHDR regime. The inclusion of all these fundamental processes effectively models the behavior of ions inside IC. The simulation is tested for proton, helium and carbon

beams and validated against Jaffe's theory for initial recombination and Boag's theory for volume recombination in pulsed and continuous beams in conventional dose rates. The parameters used in the calculations of both theories were obtained through fitting them to experimental data obtained from several experimental campaigns at different irradiation facilities measured with a plane parallel IC (Rossomme et al., 2017).

2. Materials and methods

The distribution of charge carriers created by an incident radiation particle is modeled using Jaffe's theory for initial recombination in combination with Boag model for volume recombination and the extended versions which account for the free electron fraction. The simulation methodology will follow the approach proposed by (Garciá et al., 2021): the algorithm starts by placing the charge carriers inside the active volume of the chamber. Every time step, the charges are shifted to account for the different transport processes, then the Monte Carlo algorithm to simulate recombination takes place for every ion in the simulation. To simulate initial recombination only one track is computed and developed in the simulation, whereas for volume recombination various tracks are added in different time distributions, depending on the time structure of the beam. The previous steps are repeated until all charge carriers have been collected. At the end of the simulation, the number of ions reaching the electrodes are counted, and k_s is computed as the number of ions initially created divided by the number of ions collected by the electrodes.

The non-homogeneous distribution of charge carriers created by ion beams does not allow the reduction of the dimensions of the problem. Therefore, the simulation is carried out in 3D. For modeling k_s of a specific beam, it is necessary to provide the beam's LET, dose rate, chamber geometry and voltage applied. Further details about the distribution of charge carriers, the transport process, the Monte Carlo algorithm and the dose rate implementation are given in the following sections (2.1 – 2.4).

The calculation of the k_s value and the type A uncertainties can be obtained by iterating the simulation several times, with different initial ion pair distributions created randomly by the algorithm. The uncertainty of the Monte Carlo simulation is calculated as the standard deviation of all k_s divided by the square root of the number of iterations. To calculate k_s for initial recombination, a minimum of 1000 iterations were conducted to achieve accurate results (see figure 1), resulting in uncertainties lower than 0.2% in all cases. For volume recombination and high LET beams, where a large number of ions are simultaneously present in the simulation, a dramatically reduced number of iterations is needed.

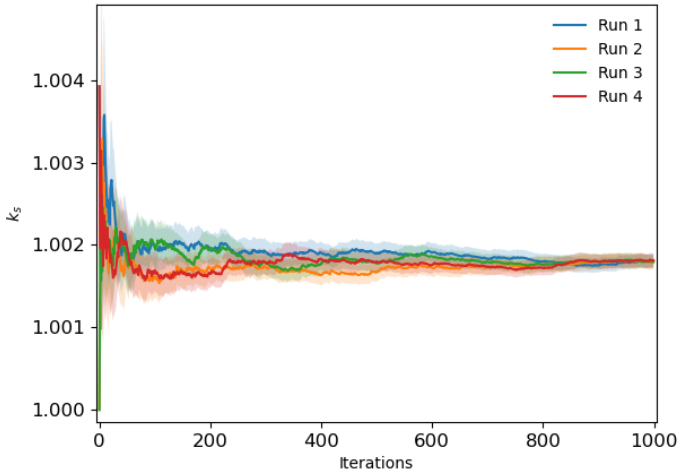

Figure 1: Evolution of various collecting histories of the k_s averaged and standard deviation bands of the mean over the number of iterations for a proton beam with 500 ions/track at 300V. The number of iterations needed to achieve a stable result is inversely proportional to the number of ions present in the simulation. The different runs converge to the same value.

The present algorithm is implemented in python. The simulation of a single track of ions of a 96 MeV proton beam in a space gap of 2mm at 300V, iterated 1000 times takes 117 *s* with a single threaded laptop with Intel i7 processor, 2.5GHz and 32GB RAM. Simulation time of volume recombination depends on the dose rate. One single iteration of the previous pulsed beam at the same voltage and a dose rate per pulse of $2.9 \cdot 10^9$ particles/s takes 205s.

2.1. Implementation of the charge carrier distribution on a single track

When the incident particle passes through the detector and ionizes the sensitive material in its track, it creates a non-homogeneous distribution of positive and negative charge carriers. Based on Jaffe's theory for column recombination (Jaffé, 1913), the charge carriers in the simulation follow a cylindrical distribution with a radial gaussian profile (see figure 2) with the width of $b^2 = 2\sigma^2$ centered at the trajectory of the incoming particle. This gaussian charge carrier density $n_0(r)$ is proved to be the best correlation with experimental data (Kaiser et al., 2012) and is modeled as:

$$n_0(r) = \frac{N_0}{\pi b^2} e^{-\frac{r^2}{b^2}} \qquad (2)$$

where N_0 is the linear charge carrier density that can be obtained as the ratio between the LET of the particle beam and the mean energy expended to form an ion pair in air by the incident radiation particle ($\overline{w}_{air}$). The parameter *b* is the initial mean square radius, which can be provided by the user, or if it is unknown, it can be calculated with the LET of the particle with the following experimental relation (Rossomme et al., 2017):

$$b\ (\cdot 10^{-3} cm) = -0.393 \cdot \log[10^{-3} \cdot LET(KeV/\mu m)]^2 + 3.094 \cdot \log[10^{-3} \cdot LET(KeV/\mu m)] - 0.584 \quad (3)$$

For low LET values, b is considered as a constant value of 10 μm (Kanai et al., 1998). For high LET values b reaches a saturation value of 50 μm (Rossomme et al., 2017).

The number of ions placed in each ion track can be calculated as the product of N_0 and the length of the particle path inside the ionization chamber. Assuming that the ionizing particle enters perpendicular to the ionization chamber, the length of the particle path is equal to the air gap size of the plane parallel chamber.

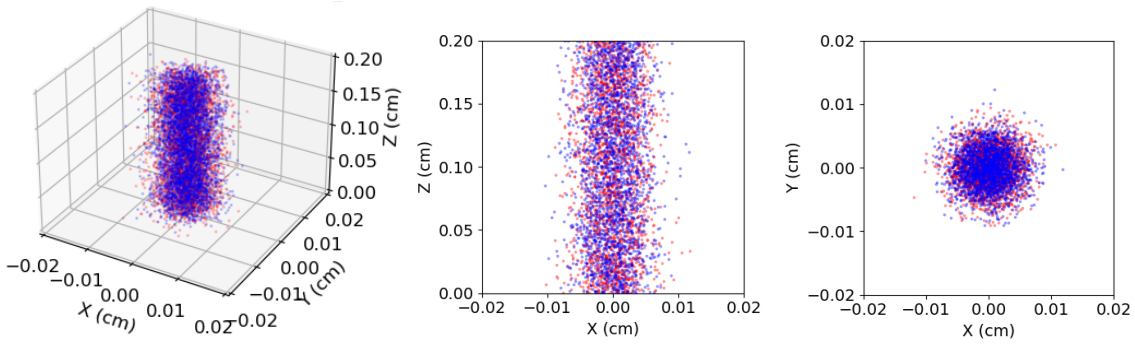

Figure 2: 3D (left), axial (center) and transversal (right) view of the gaussian structure of a 115MeV/n Carbon ion track. The blue points represent the negative charge carriers and the red points represent the positive charge carriers.

The negative charge carriers initially created by an incident particle consist of electrons. The negative ions will be formed when the electrons diffuse and attach to other molecules. Previous studies (Christensen et al., 2016) and (Paz-Martín et al., 2022) have shown that recombination between electron and positive ions is negligible for ion beams as electrons are dragged out to the collecting electrodes orders of magnitude faster than the ions. Based on this, the electrons are not added to the simulation, and the free electron fraction is considered as a lack of negative ions. Taken this into consideration, p is calculated from the parametrization in (Laitano et al., 2006), and the three different models described by Boag (Boag et al., 1996) are implemented in the simulation as:

- *Model I*: The fraction of negative ions is reduced by a factor $1 - p$.
- *Model II*: Negative ions reduced by a factor $1 - p$ are distributed in the volume of the chamber between $z = pd$ and $z = d$.
- *Model III*: A fraction of negative ions $\sqrt{1-p}$ is distributed between $z = \left(1 - \sqrt{1-p}\right)d$ and $z = d$.

2.2. Implementation of transport algorithm

After the ions are placed inside the simulation, the ions are shifted in a straight line of distance $\Delta r_{\pm}$ each time step:

$$\Delta r_{\pm}(\Delta t) = \pm\, \mu_{\pm} E \Delta t \pm^{*} \sqrt{2 D_{\pm} \Delta t} \mp \mu_{\pm} E_{SCS,i} \Delta t \qquad (4)$$

The first term models the drift of ions, which depends on the mobility of positive and negative ions ($\mu_{\pm}$) and the electric field E. In a plane parallel geometry it is assumed to be constant and it is calculated as $\frac{V}{d}$, where V is the bias applied voltage and d is the separation between plates. The time step Δt is calculated as:

$$\Delta t = \frac{b}{\delta \cdot E \mu_{\pm}}$$

where δ is the number of discretizations in the time step, which may be adjusted by choosing a value > 1 to increase the time step resolution. The second term in eq. (4) represents the diffusion motion, which is implemented with the mean squared displacement of the Brownian motion, $\overline{x^2} = 2 D_{\pm} \Delta t$. $D_{\pm}$ represents the ion diffusion constant of the negative or positive ions. Note that the sign $\pm^{*}$ in eq. (4) does not mean that the diffusion is always towards the same direction. A random positive or negative number is sampled to generate the random direction. By doing this, the ions move randomly and eventually that leads to a naturally diffusion towards lower concentration of ions. This term may produce that some charge carriers may go out of the lateral limits of the detector. In this case, they are equally collected and counted, with this we ensure that all the ions missing are due to recombination losses.

The third term corresponds to the space charge screening. It can be understood as a reduction of the electric field that the ions experiment due to the presence of other charged species that screen the electric field caused by the difference of potential between the electrodes. This term can increase recombination as the charge carriers of opposite sign overlap longer. This is implemented with a term similar to the drift but with a perturbated "screened" electric field $E_{SCS,i}$ for every positive and negative ion i. The screened electric field experienced by the ion is only taken into consideration for the z axis, which is the only vectorial component which can disturb the bias electric field in plane parallel geometry. If each track of ions is considered a cylinder of uniform charge density, the electric field is computed by integrating the contribution of each disc of the cylinder to the coordinates of the ion.

The values of the different constants used in the simulation can be found in table 1.

Constant	Symbol	Value	Units	Reference
Average ion diffusion	$D_{\pm}$	0.037	cm^2/s	(Kanai et al., 1998)
Average ion mobility	$\mu_{\pm}$	1.65	$cm^2/V \cdot s$	(Boag et al., 1996)
Ion recombination constant	α	$1.6 \cdot 10^{-6}$	cm^3/s	(Boag, 1950)

Mean energy to form an ion par	$\bar{w}_{air}/_{e}$	34.23 (protons) 35.72 (heavy ions)	J/C	(Andreo et al., 2001)
Air density	ρ	0.001225	g/cm^3	(Johnson et al., 1976)

Table 1: Parameters of the different constants used in the simulation. The use of the same diffusion and mobility parameters for positive and negative ions instead of more recent and accurate values such as (Boissonnat et al., 2016) *is justified as in this work the simulation is compared with fixed values in Jaffe and Boag theories which do not account for this distinction.*

2.3. Implementation of recombination scheme

The recombination is considered as a random process computed with a Monte Carlo scheme similar to (García et al., 2021) with some modifications which allow to reduce the computation time (see figure 3). The probability of recombination for the i-esime negative ion belonging to track k, on time step t is calculated as:

$$P_{-,i}(t) = 1 - e^{-\alpha \cdot \rho_{+,k}(t) \cdot \Delta t} \qquad (5)$$

Where $\rho_{+,k}(t)$ is the local density of positive ions in the core of track k. $\rho_{+,k}(t)$ is calculated every time step as the number of positive ions inside a sphere of radius r_f, centered in the middle of track k divided by the volume of the sphere. The value of r_f is left as a free parameter, that is found to be optimal if it is set to $1.6\frac{b}{\sqrt{2}}$ according to the best fit to the Jaffe theory for a 62 MeV/n carbon ion beam (Rossomme et al., 2016). To avoid recombination between ions that are far apart the following constrain is added: if the distance between ions is bigger than r_f, the ions do not recombine.

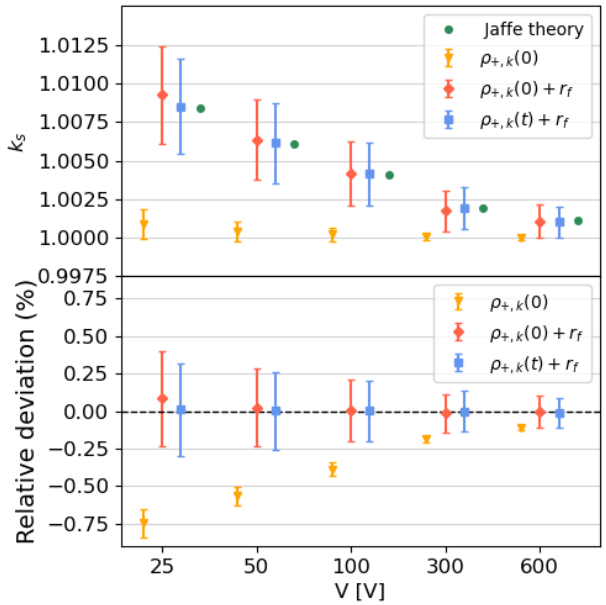

Figure 3: Relative deviation of the k_s values with Jaffe theory for different voltages when different approaches to calculate $P_{-,i}(t)$ are taken to calculate initial recombination. In yellow triangles no

radius of action r_f is considered and $\rho_{+,k}$ is calculated for each track only at the beginning of the simulation. This is equivalent to the simplified Monte Carlo algorithm in (García et al., 2021)*. In red diamonds the radius of action is included and $\rho_{+,k}$ is calculated only at the beginning of the simulation. In blue squares the radius of action is included and the probability is calculated on each time step for each track. This last approach satisfactorily predicts the theoretical values with minimal relative difference, less than 0.01% for initial recombination in a proton beam.*

2.4. Implementation of dose rate for volume recombination

To model initial recombination, one track is added and evolved in the simulation. For volume recombination the same scheme is followed but various tracks (N_{tracks}) are placed randomly in the area of the simulation (πr_{sim}^2) according to the fluence rate ($\dot{\varphi}$) that depends on the dose rate ($\dot{D}$) as proposed by (Christensen et al., 2016):

$$N_{tracks} = \pi r_{sim}^2 \dot{\varphi}, \quad \dot{D} = \dot{\varphi}\left(\frac{\bar{S}_{en}}{\rho_{air}}\right) \tag{6}$$

The number of tracks needed to add to the simulation and their distribution over time depends on the dose rate and if the beam is considered pulsed or continuous. A beam is considered pulsed when the amount of time needed to collect all the ions inside the volume of the ionization chamber is much shorter than the pulse repetition period and if the pulse duration is much shorter than the collection time of the IC. Considering this definition, the pulsed beam is simulated by inserting all tracks in the simulation homogeneously along the pulse duration and considering the instant dose rate of the pulse. A continuous beam is considered when the beam does not fulfill the previous definition. In this case, the average dose rate is considered and the tracks are inserted following a homogeneous distribution over the simulation time. Due to computation limitations, only a fraction of the ionization chamber volume is simulated ($r_{sim} \sim r_{IC}/10$). Figure 4 shows how the ion tracks are sampled all over the area of the simulation according to the different dose rates.

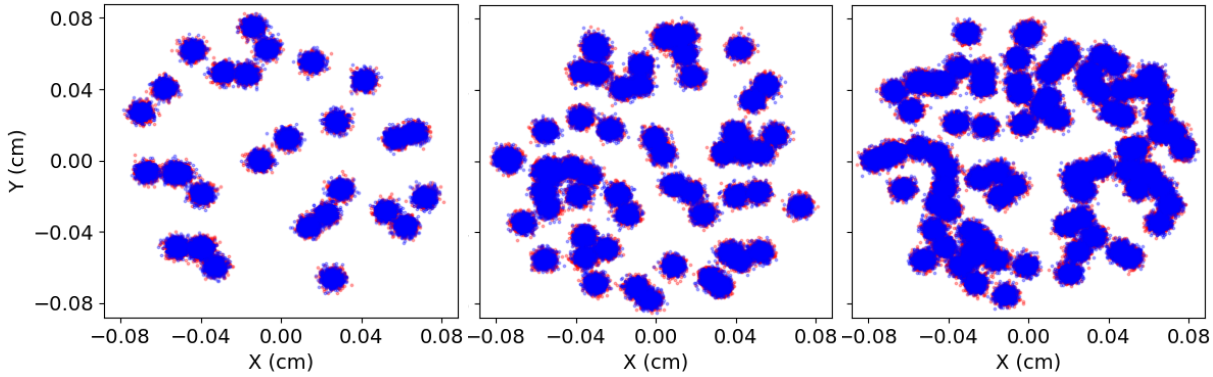

Figure 4: Distribution of Carbon Ion tracks over the transversal section of the IC for 3 dose rates (DR): 0.3·DR, 0.6·DR and DR (corresponding to ~16Gy/min) of a continuous Carbon Ion Beam [from left to right]. Each cluster of points represents a column of ions as shown in Figure 2.

2.5. Experimental setup for code validation

To validate the numerical code, k_s values for different beams and voltages were computed based on parameters from published experimental data for proton, helium and carbon beams (Rossomme et al., 2017). All measurements were performed with an IBA PPC40, with an air gap size of $2mm$ over voltages ranging $20 - 600V$. Through the Jaffe plots and fittings to Boag and Jaffe models, theoretical k_s values were determined and compared with our numerical results.

A $96.17\ MeV$ non-modulated pulsed pencil beam scanning (PBS) proton beam produced by a synchro-cyclotron was used. The pulsed repetition frequency was $1kHz$ and the pulse length varied between $4 - 6\ \mu s$. Heavier ion beams in continuous mode were also investigated. A $50.57\ MeV/n$ PBS helium beam produced by a synchrotron. The spill duration was in the range of $5\ s$ and the pause between spills was $4.5\ s$. A $115\ MeV/n$ PBS carbon ion beam produced by synchrotron, with spill duration between $1 - 3\ s$ and pause between spills $4.5\ s$. More details can be found in (Rossomme et al., 2017).

3. Results and validation

3.1. Proton beam

For the $96.17\ MeV$ pulsed proton beam, the parameters used to model the track structure were: $N_0 = 2559\ ions/cm$ and $b = 0.00225\ cm$ according to the values that can be found in (Rossomme et al., 2017). In figure 5 (a) it can be seen that the results for initial recombination are in good agreement with Jaffe theory, the relative differences between theoretical values and the Monte Carlo simulation for the different voltages were below 0.05%.

In figure 5 (b), results for six doses per pulse were compared to verify that the simulation can satisfactorily compute volume recombination for the following dose rates: $0.5 * DR, DR, 1.7 * DR, 1.92 * DR, 3.33 * DR$ and $6.21 * DR$, with DR the dose rate per pulse corresponding to $2.9 \cdot 10^9$particles per pulse. Volume recombination can be calculated independently if the condition of only allow recombination between ions from different tracks is added. To calculate both volume and initial recombination at the same time in the simulation, no constraint is added. All the computed k_s values are in accordance with Boag theory. If the free electron fraction (e.g. *p*=0.24 at 300V) is considered, small relative differences were found only at high voltages: at 500V, 0.05% with Boag model I, 0.08% with Boag model II and 0.07% with Boag model III. As there is no consensus on which model is the most accurate and the relative difference were very small, no free electron fraction was considered. Similar differences were found for all the other cases shown in this work. Values of the uncertainty were found to be 0.02% or smaller.

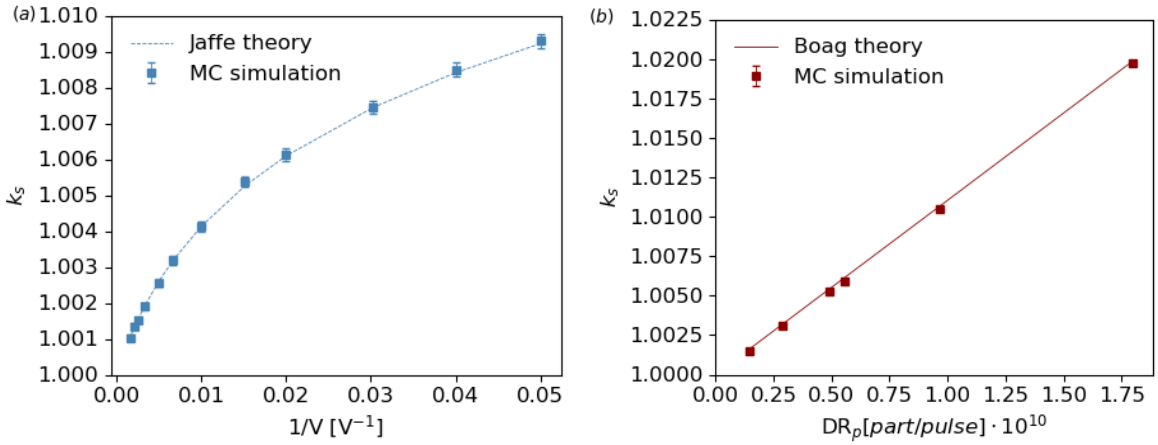

Figure 5: (a) k_s versus inverse of the voltage for a $96.17\ MeV$ proton beam. Comparison between Jaffe theory (blue dashed line) and Monte Carlo simulation (blue solid squares) for initial recombination. (b) k_s versus the dose rate per pulse (DR_p) at 300V. Comparison between Boag (red solid line) and Monte Carlo simulation (red solid squares) for volume recombination in a pulsed proton beam.

3.2. Helium beam

For the $50.57\ MeV/n$ Helium beam, the parameters used for the track in the simulation were: $N_0 = 1739\ ions/cm$ and $b = 0.00137\ cm$ according to the calculations that can be found in (Rossomme et al., 2017). At 0.67 cm water equivalence depth (in the plateau) three dose rates were used: $DR, 0.66 * DR$ and $0.5 * DR$. For this beam, the absolute dose rate values within the phantom were not available due to the complexity of the definition of the dose rate in PBS modalities. (Rossomme et al., 2017) primarily relied on the relative values, which is similarly done in this work by scaling the dose rate values. In the pulsed proton beam from previous section, it was possible to validate the k_s values related to certain levels of dose rate. These values served to obtain a rough estimation of the dose rate levels of the other beams according to eq. (6). In this case, the average dose rate (DR) was found to be of order of $3\ Gy/min$.

Figure 6 (a) shows a comparison between numerical and theoretical k_s-values for the three dose rates. The uncertainty values ranged from 0.05% to 0.01%, the highest values were found for the initial recombination or low dose rates where less ions are involved.

In Figure 6 (b), numerical values are compared to theoretical values for the dose rate DR, when initial and volume recombination are both present and their contribution. The total theoretical k_s is calculated as the product of Jaffe theoretical value and Boag theoretical value: $k_{s,Theo}^{ini\ \&\ vol} = k_{s,Jaffe}^{ini} \cdot k_{s,Boag}^{vol}$.

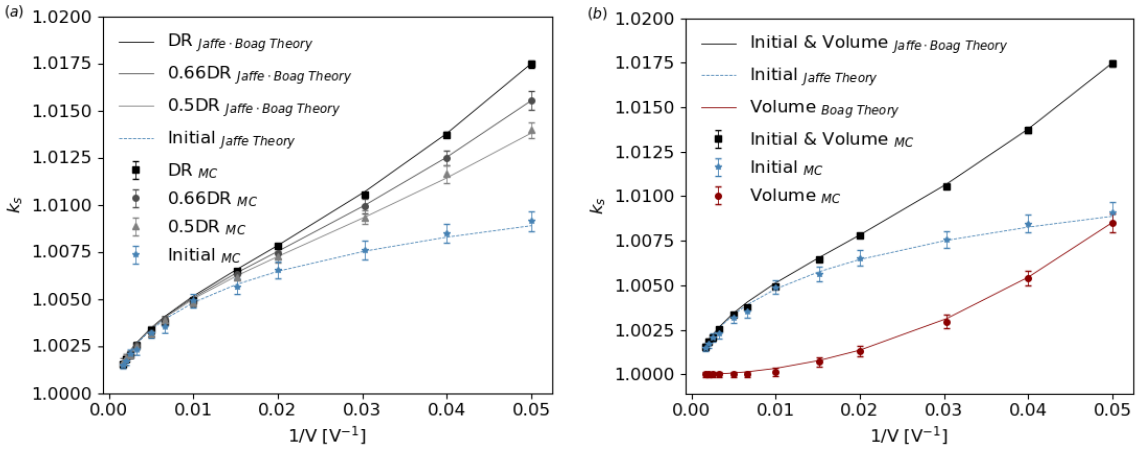

Figure 6: (a) Comparison between theoretical values on solid curves and MC simulation on solid symbols for three different dose rates: $DR, 0.66 * DR$ and $, 0.5 * DR$ with the contribution from initial recombination (blue). (b) Contribution of initial and volume recombination (for the dose rate DR) to the total k_s versus inverse of the voltage for a $50.57\ MeV/n$ Helium beam. The solid red circles show the MC calculation of the volume recombination contribution and on solid red curve the theoretical values from Boag theory. The solid blue stars show the MC calculation of initial recombination and on the dashed blue curve the theoretical values from Jaffe theory. The solid black squares show the MC calculation of the total recombination and on the solid black curve the theoretical values that can be obtained from multiplying Jaffe and Boag theories.

3.3. Carbon beam

To model a $115\ MeV/n$ Carbon Ion beam in the plateau, the parameters used in the simulation were: $N_0 = 9565\ ions/cm$ and $b = 0.00345\ cm.$ Figure 7 (a) shows k_s values for the three dose rates tested: DR, $0.6 * DR$ and $0.3 * DR$. As done for the helium beam (see section 3.2), the average dose rate (DR) was estimated to be $16\ Gy/min$ following the same estimation as in Section 3.2. To model the same beam in the middle of the SOBP the parameters used in the simulation were: $N_0 = 15478\ ions/cm$ and $b = 0.0037\ cm.$ Figure 7 (b) shows the tested dose rates: DR and $0.6 * DR$, where $DR \approx 26\ Gy/min$. All the results are in accordance with theoretical values. Values of the uncertainty were found to be 0.1% or smaller.

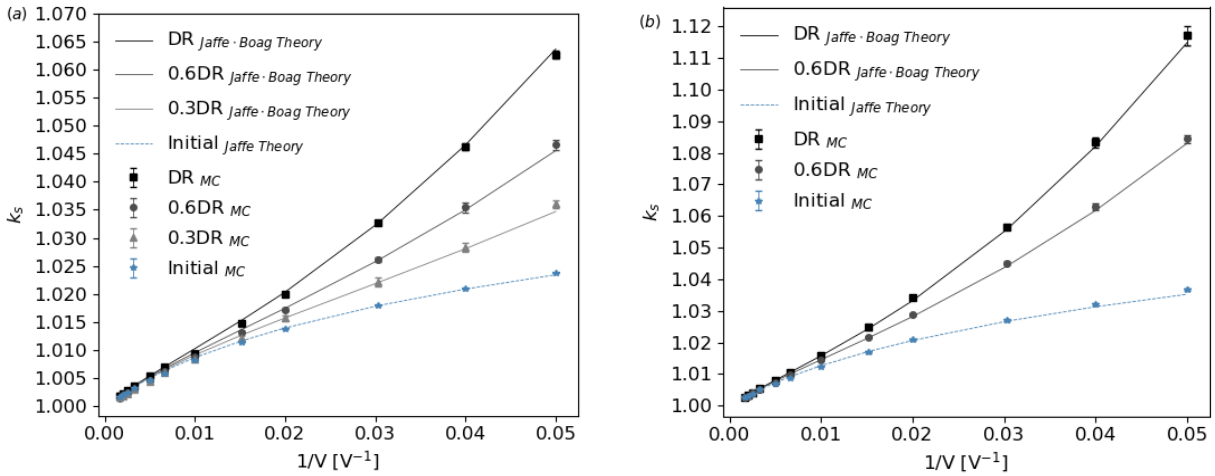

Figure 7: k_s versus inverse of the voltage of a 115 MeV/n Carbon ion beam. (a): Comparison between Jaffe, Boag theoretical values (solid lines) and numerical values (symbols) for different dose rates at the plateau. (b): Analogous graph for the Spread Out Bragg Peak (SOBP).

4. Discussion and conclusion

In this study, we have presented a Monte Carlo simulation code that effectively models the ion recombination factor for plane parallel ionization chambers exposed to ion beams. Our simulation demonstrated excellent agreement with established theories, such as Jaffe theory for initial recombination and Boag theory for volume recombination, across various ion beams, including continuous helium, carbon and pulsed proton beams, regardless of the temporal structure of the beam.

We have also introduced a novel approach to compute recombination, significantly reducing simulation time compared to previous work. This enables three-dimensional calculations necessary to model initial recombination and its interplay with volume recombination in a reasonable time. While our implementation considered effects like diffusion, free electron fraction and space charge screening, validation with experimental data showed that the free electron fraction and the space charge screening term are negligible due to the low dose rates and dose per pulse conditions addressed in this work.

However, as the dose rate increases, the Boag theory is not in accordance with the simulated values. This trend, previously observed (Paz-Martín et al., 2022), suggests that Boag theory is not suitable for UHDR conditions due to the non-inclusion of the space charge screening. Figure 8 (a) illustrates the difference in k_s values with and without the inclusion of space charge. It is predicted that for PPC40, Boag theory will start to fail if the dose rate per pulse is increased by approximately one order of magnitude compared to the dose rates in the pulsed proton beam used in this work. Figure 8 (b) shows the distortion of the electric field along the IC air gap according to the distribution of ions proposed in Boag model II. At low dose rates (as used in this work), the screened electric field is negligible. As the dose per pulse increases, the electric field

becomes more and more screened with a linear dependence with the dose rate. A 10% relative difference in k_s value was found at $4.25 \cdot 10^{11}$ part/pulse, where the maximum distorted electric field reaches 600 V/cm, representing a 40% difference from the bias voltage.

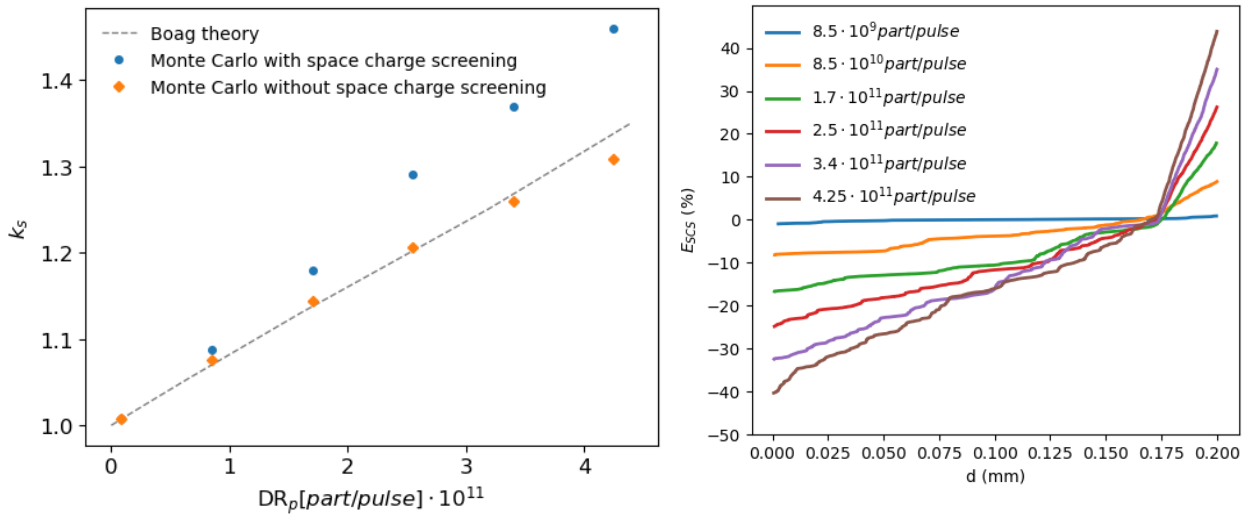

Figure 8: (a) k_s versus the dose rate per pulse (DR_p) at 300V for a pulsed proton beam. Comparison between Boag theory (dashed gray line) and Monte Carlo simulation if the space charge screening is included in the simulation (blue solid circles) and if the space charge screening effect is not included in the simulation (orange solid diamonds). (b) Distortion of the electric field relative to the bias electric field (1500 V/cm) along the air gap for different dose rates according to Boag distribution of free electrons II.

Further investigations with experimental values are needed to benchmark the simulation in the ultra-high dose rate regime where Boag theory fails. This simulation tool holds the potential to extend k_s calculations beyond these limits. Other effects, such as the charge multiplication, should be further investigated as it could potentially interplay with the free electron fraction and space charge screening.

Bibliography:

This work is supported by the Walloon Region under the project name D-CAF (Dosimetry for Carbon, ARC and FLASH therapies), MecaTech Appel 31.

The authors thank Antonio Miguel Lallena Rojo for his valuable insights during the initial stage of this work, as well as Daniel Plaza Vas for the technical discussions that aided in refining key aspects of the simulation.

Bibliography:

Almond, P., Biggs, P., Coursey, B., Hanson, W., Huq, M., Nath, R., & Rogers, D. (1999). AAPM's TG-51 protocol for clinical reference dosimetry of high-energy photon and electron beams. In *Medical Physics (Lancaster)*. https://doi.org/10.1118/1.598691

Andreo, P., Burns, D. T., Hohlfeld, K., Kanai, T., Laitano, F., & Smyth, V. (2001). *Absorbed Dose Determination in External Beam Radiotherapy: An International Code of Practice for Dosimetry based on Standards of Absorbed Dose to Water*.

Boag J W. (1950). Ionization measurements at very high intensities. Pulsed radiation beams. *British Journal of Radiology*. https://doi.org/10.1259/0007-1285-23-274-601

Boag, J. W., Hochhäuser, E., & Balk, O. A. (1996). The effect of free-electron collection on the recombination correction to ionization measurements of pulsed radiation. In *Phys. Med. Biol* (Vol. 41). http://iopscience.iop.org/0031-9155/41/5/005

Boissonnat, G., Fontbonne, J. M., Colin, J., Remadi, A., & Salvador, S. (2016). Measurement of ion and electron drift velocity and electronic attachment in air for ionization chambers. In *arXiv: Instrumentation and Detectors*.

Boutillon, M. (1998). Volume recombination parameter in ionization chambers. In *Physics in medicine and biology*. https://doi.org/10.1088/0031-9155/43/8/005

Christensen, J. brage, Tölli, H., & Bassler, N. (2016). A general algorithm for calculation of recombination losses in ionization chambers exposed to ion beams. *ArXiv: Medical Physics*. https://doi.org/10.1118/1.4962483

García, L. I. R., Pérez-Azorín, J. F., Anguiano, M., & Lallena, A. M. (2021). Monte Carlo calculation of charge collection efficiencies in ionization chambers. *Physics in Medicine and Biology*. https://doi.org/10.1088/1361-6560/ABD4F8

Garciá, L. I. R., Pérez-Azorín, J. F., Anguiano, M., & Lallena, A. M. (2021). Monte Carlo calculation of charge collection efficiencies in ionization chambers. *Physics in Medicine and Biology*, *66*(4). https://doi.org/10.1088/1361-6560/abd4f8

Huxley, L. G. H. and R. W. C. (1974). *Diffusion and drift of electrons in gases* (John Wiley and Sons, Ed.). Wiley Series in Plasma Physics.

Jaffé, G. (1913). Zur Theorie der Ionisation in Kolonnen. *Annalen Der Physik*. https://doi.org/10.1002/ANDP.19133471205

Johnson, D. L., Roberts, B. C., & Vaughan, W. W. (1976). *Reference and standard atmosphere models*.

Kaiser, F.-J., Bassler, N., Tölli, H., & Jäkel, O. (2012). Initial recombination in the track of heavy charged particles: Numerical solution for air filled ionization chambers. *Acta Oncologica*. https://doi.org/10.3109/0284186X.2011.626452

Kanai, T., Sudo, M., Matsufuji, N., & Futami, Y. (1998). Initial recombination in a parallel-plate ionization chamber exposed to heavy ions. In *Phys. Med. Biol* (Vol. 43). http://iopscience.iop.org/0031-9155/43/12/012

Laitano, R. F., Guerra, A. S., Pimpinella, M., Caporali, C., & Petrucci, A. (2006). Charge collection efficiency in ionization chambers exposed to electron beams with high dose per pulse. In *Physics in medicine and biology*. https://doi.org/10.1088/0031-9155/51/24/009

Niatel, M. T. (1967). An experimental study of ion recombination in parallel-plate free-air ionization chambes. *Physics in Medicine and Biology*. https://doi.org/10.1088/0031-9155/12/4/009

Palmans, H., Thomas, R., & Kacperek, A. (2006). Ion recombination correction in the Clatterbridge Centre of Oncology clinical proton beam. In *Physics in medicine and biology*. https://doi.org/10.1088/0031-9155/51/4/010

Paz-Martín, J., Schüller, A., Bourgouin, A., González-Castaño, D. M., Gómez-Fernández, N., Pardo-Montero, J., Gómez, F., Paz-Martín, J., Schüller, A., Bourgouin, A., González-Castaño, D. M., Gómez-Fernández, N., Pardo-Montero, J., & Gómez, F. (2022). *Numerical modeling of air-vented parallel plate ionization chambers for ultra-high dose rate applications*. https://doi.org/10.1016/J.EJMP.2022.10.006

Rossomme, S., Delor, A., Lorentini, S., Vidal, M., Brons, S., Jkel, O., Cirrone, G. A. P., Vynckier, S., & Palmans, H. (2020). Three-voltage linear method to determine ion recombination in proton and light-ion beams. *Physics in Medicine and Biology*, *65*(4). https://doi.org/10.1088/1361-6560/ab3779

Rossomme, S., Hopfgartner, J., Lee, N. D., Delor, A., Thomas, R. A. S., Romano, F., Fukumura, A., Vynckier, S., & Palmans, H. (2016). Ion recombination correction in carbon ion beams. *Medical Physics*, *43*(7), 4198–4208. https://doi.org/10.1118/1.4953637

Rossomme, S., Horn, J., Brons, S., Jäkel, O., Mairani, A., Ciocca, M., Floquet, V., Romano, F., Rodriguez Garcia, D., Vynckier, S., & Palmans, H. (2017). Ion recombination correction factor in scanned light-ion beams for absolute dose measurement using plane-parallel ionisation chambers. *Physics in Medicine and Biology*, *62*(13), 5365–5382. https://doi.org/10.1088/1361-6560/aa730f